Real-time Semi-automatic Segmentation of Hepatic

(a)

TABLE I. COMPARISON BETWEEN MANUAL AND SEMI-AUTOMATIC METHODS FOR RFA LESION SEGMENTATION

	Number of lesions	Correlation coefficient (%)	Average error (mm^2)	Max error (mm^2)	Intra-observer coefficient of variation (%)	Inter-observer coefficient of variation (%)	Average segmentation time per lesion (min)
Exposed Liver							
Manual segmentation	11	84.6	25.7	87.4	1.8	5.3	3.9
Algorithm	11	96.5	12.3	33.2	0.4	0.9	0.2
Transcutaneously							
Manual segmentation	3	-	128	321	3.2	9.0	3.8
Algorithm	3	-	25.7	52.7	0.4	2.6	0.2

Matched sonoelastographic, B-mode and gross pathology images are presented in Fig. 1. An RFA lesion is found at the top left of the sonoelastographic image next to a vessel. The corresponding B-mode image shows a hyperechoic region due to the gas bubbles formed by the RFA process. The area of the hyperechoic regions does not correspond to the area of the actual lesion. The gross pathology image confirms the presence of the lesion next to a vessel which has collapsed after the liver was excised.

A comparison between manual and semi-automatic segmentation is illustrated in Fig. 2. Three independent observers manually drew different outlines for the same lesion. The same observers initialized the semi-automatic algorithm by picking the center of the lesion. Even though they picked different centers, the algorithm produced the same outline.

Fig.3 depicts an example of a sonoelastographic image obtained transcutaneously and the outline of the lesion generated by the semi-automatic algorithm. In general, these images presented a lower signal-to-noise ratio (SNR) when compared to exposed liver results.

IV. DISCy(r)-21(SC)SCy(r)-24(r)-24(r)-24 0 7.92 1n7-0.010l23(p)9(s)nc TfCy(r)-210 Td (-1.071 TD [(T512(obt)-4.9053(p) 1 Tf 0-15((ed)

principles, techniques, and diagnostic imaging guidance," AJR. Am. J. Roentgenol., vol. 174, pp.323–331, 2000.

[3] L. Solbiati, T. Ierace, S.N. Goldberg, S. Sironi, T. Livraghi, R. Fiocca, et al., "Percutaneous US-guided radio-frequency tissue ablation of liver metastases: Treatment and follow-up in 16 patients," Radiol., vol. 202, pp. 195-203, 1997.

[4] L. Solbiati, S.N. Goldberg, T. Ierace, T. Livraghi, F. Meloni, M. Dellanoce, et al., "Hepatic metastases: Percutaneous radio-frequency ablation with cooled-tip electrodes," Radiol., vol. 205, pp. 367-373, 1997.

[5] M. Zhang, "The measurement and imaging of viscoelastic properties of soft tissues and lesions," Ph.D. Dissertation, University of Rochester, 2007.

[6] J. Hindley, W.M. Gedroyc, L. Regan, E. Stewart, C. Tempany, K. Hynyen, et al., "MRI guidance of focused ultrasound therapy of uterine fibroids: Early results," AJR. Am. J. Roentgenol., vol. 183, pp. 1713-1719, 2004.

[7] C.H. Cha, F.T. Lee, J.M. Gurney, B.K. Markhardt, T.F. Warner, F. Kelcz, et al., "CT versus sonography for monitoring radiofrequency ablation in a porcine liver," AJR. Am. J. Roentgenol., vol. 175, pp. 705-711, 2000.

[8] S.A. Curley, "Radiofrequency ablation of malignant liver tumors.," Oncologist., vol. 6, pp. 14-23, 2001.

[9] T. Varghese, U. Techavipoo, W. Liu, J.A. Zagzebski, Q. Chen, G. Frank, and F.T. Lee Jr., "Elastographic measurement of the area and volume of thermal lesions resulting from radiofrequency ablation: Pathologic correlation," AJR. Am. J. Roentgenol.; vol. 181, pp. 701-707, 2003.

[10] R.M. Lerner, K.J. Parker, J. Holen, R. Gramiak, and R.C. Waag, "Sonoelasticity: Medical elasticity images derived from ultrasound signals in mechanically vibrated targets," Acoust. Imaging, vol. 16, pp. 317-327, 1998.

[11] S.R. Huang, R.M. Lerner and K.J. Parker, "On estimating the amplitude of harmonic vibration from the Doppler spectrum of reflected signals," J. Acoust. Soc. Am., vol. 88, pp. 310-317, 1990.

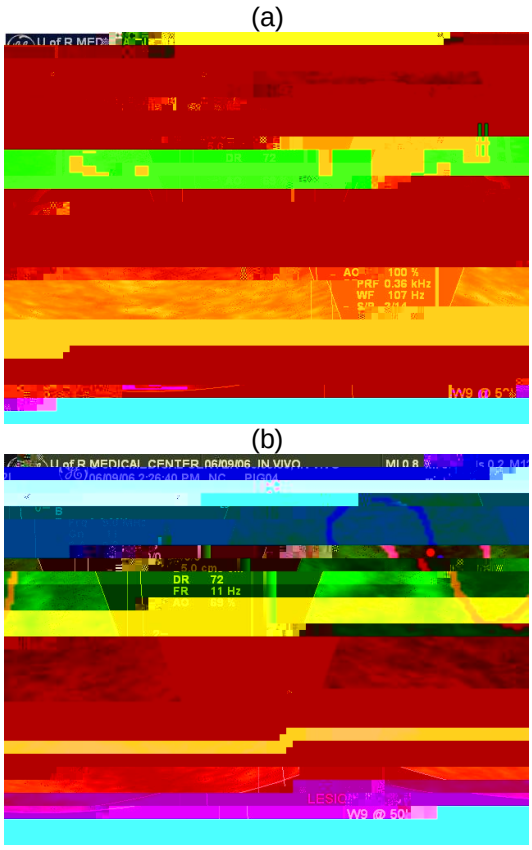

Figure 2. Comparison between (a) Manual and (b) Semi-automatic segmentation. Three independent observers (shown in blue, pink and violet) manually outlined the lesion and selected the center of the lesion to initialize the semi-automatic algorithm.

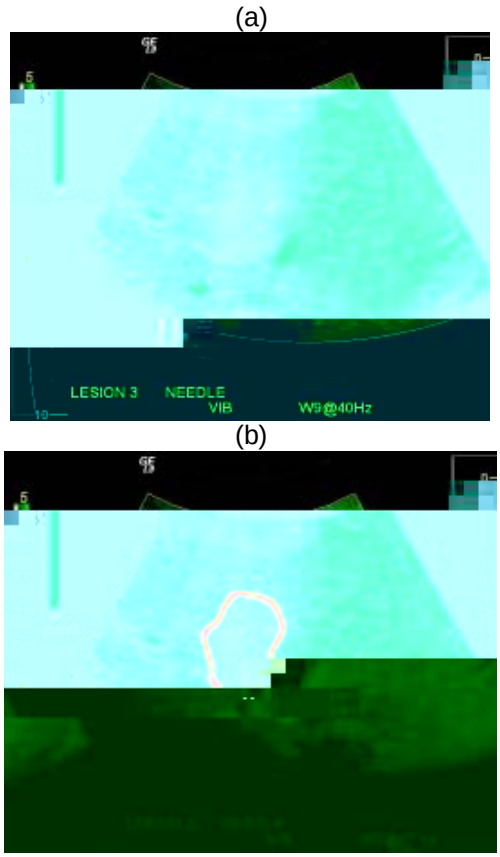

Figure 3. (a) Sonoelastographic image of an RFA lesion created transcutaneously and (b) Segmentation performed by the semi-automatic algorithm.